Journal of Power Sources 196 (2011) 2373–2379

Contents lists available at ScienceDirect

Journal of Power Sources

journal homepage: www.elsevier.com/locate/jpowsour

Template-free prepared micro/nanostructured polypyrrole with ultrafast charging/discharging rate and long cycle life

Jie Wang, Youlong Xu*, Feng Yan, Jianbo Zhu, Jingping Wang

Electronic Materials Research Laboratory, Key Laboratory of the Ministry of Education, Xi'an Jiaotong University, Xi'an 710049, China

ARTICLE INFO

Article history:
Received 26 August 2010
Accepted 22 October 2010
Available online 30 October 2010

Keywords:
Polypyrrole
Micro/nanostructure
Electrochemical
Template-free
Supercapacitors

ABSTRACT

A highly electroactive polypyrrole with hollow "horns" in micro/nanometers (h-PPy) is galvanostatically prepared by a template-free approach in p-toluenesulfonate alkaline solution. Its electrochemical capacitance properties are characterized to verify its promising applicability for supercapacitors. Besides its high specific surface area, h-PPy shows unexpectedly good ordering of molecular chain and great conjugation length, contributing to high ionic and electronic conductivity. These advantages lead to a remarkable specific capacitance of 400 F g^{-1} and ultrafast charging/discharging capability with a specific capacitance of 274 F g^{-1} at the charging/discharging time of even 0.4 s. Moreover, the micro/nanostructured hollow "horns", which can tolerate the mechanical stress in charging/discharging process, significantly improve the cycle life of h-PPy so that the capacitance retains 90% after 100,000 continuous cycles. All of its distinguishing quality enable h-PPy to be an excellent active material of supercapacitors.

1. Introduction

Electrochemical capacitors (also known as supercapacitors), bridging the gap between batteries and conventional dielectric capacitors in Ragone plot, are ideal devices for the rapid storage and release of energy. They not only enable electric vehicles but also provide back-up for wind and solar energy, both of which are essential to meet the challenge of global warming and the finite nature of fossil fuels [1]. Therefore, supercapacitors have attracted great attention recently [2,3]. Much research has been devoted to increasing energy and power density, as well as decreasing fabrication costs and using environmentally friendly materials [4]. Thanks to their high conductivity and large pseudo-capacitance, especially the potential to fabricate flexible solid supercapacitors, electronically conducting polymers (ECPs) have been the focus of supercapacitor studies [5–8]. Among ECPs, conducting polypyrrole (PPy) is one of the prominent electrode materials of supercapacitors due to its low cost, ease of synthesis, and environmentally friendly feature [9–12]. Despite its specific capacitance is greater than that of carbon materials in current commercial application, it is still generally beneath 300 F g^{-1} and needs further improvement to achieve higher energy density. Furthermore, its fast charging/discharging ability, restricted by low ionic mobility within the solid polymer, is under improving to achieve higher power density. Most of all, the cycle life of PPy electrode is limited, like that of other ECPs, because of the repeating contraction and expansion of the electrode in cycling process. Therefore, the performance of PPy electrode needs to be enhanced substantially to meet the higher requirement in future system ranging from portable electronics to electric vehicles and large industrial equipments.

A rational approach to fulfill the task is to synthesize micro/nanostructured PPy electrode. The micro/nanostructure can shorten the diffusion path of ions and ensure sufficient surface area and its good accessibility for the electrolyte so as to improve the specific capacitance and fast charging/discharging ability [13]. The micro/nanostructured PPy films are generally prepared by chemical and electrochemical methods, where the latter has many advantages. The most important one is that PPy films can be directly produced on the current collector and naturally integrated as continuous uniform films, saving the use of binder that is often an insulator and hydrophobic, such as polytetrafluoroethylene (PTFE).

A conventional strategy to electrochemically prepare micro/nanostructured PPy for supercapacitors is to synthesize nanocomposites of PPy and carbon nanotubes (CNTs) where CNTs play a role of one-dimension template [14–20]. The composites exhibit more excellent performance than the single ECPs and CNTs due to the nanometer size effect and synergy effect. Another strategy is to prepare pure PPy with micro/nanostructure, generally PPy nanorods, using porous membrane, such as anodized aluminum oxide (AAO), [21–23] which was first reported by Martin [24]. Recently, Lee et al. synthesized conducting polymer nanotubes via template method and demonstrated that the nanotubes-like polymer has better electrochemical capacitance performance than the corresponding nanorod-like material [25]. More information is available in an early review [26]. The template approach based on hard porous membranes, such as AAO, microporous polymeric

* Corresponding author. Tel.: +86 29 82665161; fax: +86 29 82665161.
E-mail address: ylxuxjtu@mail.xjtu.edu.cn (Y. Xu).

0378-7753/$ – see front matter © 2010 Elsevier B.V. All rights reserved.
doi:10.1016/j.jpowsour.2010.10.066

filtration membranes and particle track-etched membranes, was called hard template method, with which the size and its distribution of PPy micro/nanostructure are easy to be controlled [27]. However, it requires rather tedious preparation and removing of template. The micro/nanostructure also might be damaged during the removing process. Therefore, increasing effort has been directed toward exploring template-free or soft template (also called molecule template) methods, realized by self-assemble or self-organization of surfactant ions in the solution. It is easy to remove molecule template after the synthesis, and well protect the micro/nanostructures of polymers. Yang and Wan synthesized microtubules of PPy by an electrochemical template-free method in β-naphthalenesulfonic acid (β-NSA) solution [28]. PPy films with dishware-like microcontainers were electrochemically synthesized by a "gas bubble" template with β-NSA as the dopant, where "gas" is the electrogenerated oxygen or hydrogen [29,30].

We reported horn-like PPy (h-PPy) was electrochemically synthesized in alkaline solutions without any membranes as template. With h-PPy films as the template, a highly porous composite of poly (3,4-ethylenedioxythiophene) and h-PPy has been further electrochemically prepared, having high specific capacitance of 290 F g^{-1} and good cycle stability [6]. In this study, we investigated the growth mechanism, morphology and molecular structure of h-PPy. It was found that the horns were hollow and open during the early growth process and the molecular chains of horns had an unexpectedly good ordering and great conjugation length. The unique structure led to a high specific capacitance of 400 F g^{-1}, and an ultrafast charging/discharging ability and a long life more than 100,000 cycles. Therefore, h-PPy itself was an excellent electrode material for supercapacitors.

2. Experimental

Pyrrole monomer (Py, Alfa, 99%) was distilled prior to use. p-Toluenesulfonic acid (TOSH, China Medicine Group, AR) and the sodium p-toluenesulfonic acid (TOSNa, China Medicine Group, CP) were used as received. The electrochemical polymerization was carried out in an electrochemical cell with two tantalum (Ta) sheets (1 cm × 1 cm × 0.01 cm) as working electrode and counter electrode, respectively. The Ta substrates were mechanically polished and cleaned with acetone and deionized water. To prepare h-PPy, the electrolyte consisted of 0.3 M p-toluenesulfonate (TOS^-) and 0.3 M Py monomer, with pH = 9. The pH of the solution was monitored by an advanced pH meter, and kept constant by adding TOSH solution frequently during the polymerization. The reason why pH value will change during this process was presented in scheme SI1. As a contrast, regular PPy films with cauliflower-like morphology (denoted as c-PPy) were synthesized in 0.3 M p-toluenesulfonate ions (TOS^-) and 0.3 M Py monomer solution, with pH = 1.5. To reveal the formation mechanism of the novel horns of h-PPy, we systemically changed the polymerization condition except the temperature (0 °C), including the concentration of TOS^- and Py, the pH value of polymerization solution, the current density and polymerization time.

A Versatile Multichannel Potentiostat 2/Z (VMP2, Princeton Application Research) was used to perform all the electrochemical preparation and characterization of PPy electrodes. The electrochemical characterization was carried out in a three-electrode cell at room temperature in 3 M KCl aqueous solution, where a platinum foil serving as counter electrode, a saturated calomel electrode (SCE) as the reference electrode. The surface morphology of the PPy films was observed by a scanning electron microscopy (JEOL Model 6700). The room temperature conductivity of free-standing PPy films was tested with the four-probe method. Raman spectroscopy was obtained by LabRAM HR800 Raman microscope (Horiba Jobin Yvon). X-ray diffraction (XRD, Rigaku D/MAX 2500) using Cu Kα radiation with wavelength (λ) of 0.15405 nm was applied for the characterization of the structure.

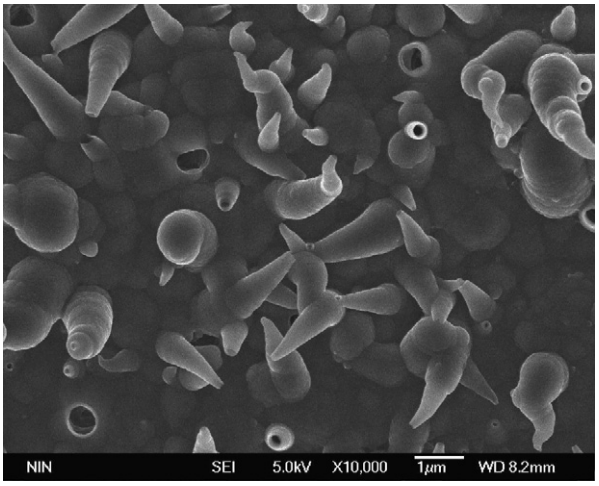

Fig. 1. SEM image of horn-like PPy synthesized with a current density of 5 mA cm^{-2} in 0.3 M TOS^- and 0.3 M Py solution with pH = 9.

3. Results and discussion

There are little report available about synthesizing PPy in alkaline solution because OH^- hinders the polymerization of pyrrole by deprotonating the cation radicals to form neutral radicals to interfere with the coupling reaction [31]. However, a novel micro/nanostructured horn-like PPy (h-PPy) films, distinguished from the typical cauliflower-like PPy films (c-PPy) synthesized in acid solution, [32] are achieved in 0.3 M TOS^- and 0.3 M Py solution with its pH = 9 at the current density of 5 mA cm^{-2} (Fig. 1). Note that the horns are hollow, which endows it with nanometer-sized transport path for ions and electrons when h-PPy is applied to supercapacitor electrodes.

To reveal the growth mechanism of the novel micro/nanostructure, we systemically investigated the effect of polymerization conditions on the formation of horn-like structure, i.e., the pH value of the solutions, the concentration of Py monomer (C_{Py}) and TOS^- (C_{TOS^-}), the current density (J) and the polymerization time. Fig. 2 presents the morphology of PPy synthesized in various conditions, which shows that the pH value of the solution is a key factor and pH = 9 is a favorable condition for h-PPy (Fig. SI1). The concentration of TOS^- greater than 0.3 M is the other essential factor, as shown by Table 1. On the contrast, Py concentration and current density have weak influence on formation of horns. In addition, the length of horn depends on polymerization time (Fig. SI3).

According to the above discussion, TOS^- and OH^- are in favor of the formation of hollow horns in h-PPy. Therefore, the growth mechanism of horns is proposed as that with its own surfactant characteristics and the assistance of OH^-, the absorbed micelles of

Table 1
Dependence of growth of the horns on polymerization condition.

pH	C_{TOS^-} 0.1 M C_{Py} (M)			C_{TOS^-} 0.3 M C_{Py} (M)			C_{TOS^-} 0.6 M C_{Py} (M)		
	0.1	0.3	0.6	0.1	0.3	0.6	0.1	0.3	0.6
1.5	n[a]	n	n	n	n	n	n	n	n
9	n	n	n	y[b]	y	y	y	y	y

[a] n: there were no horns.
[b] y: there were horns.

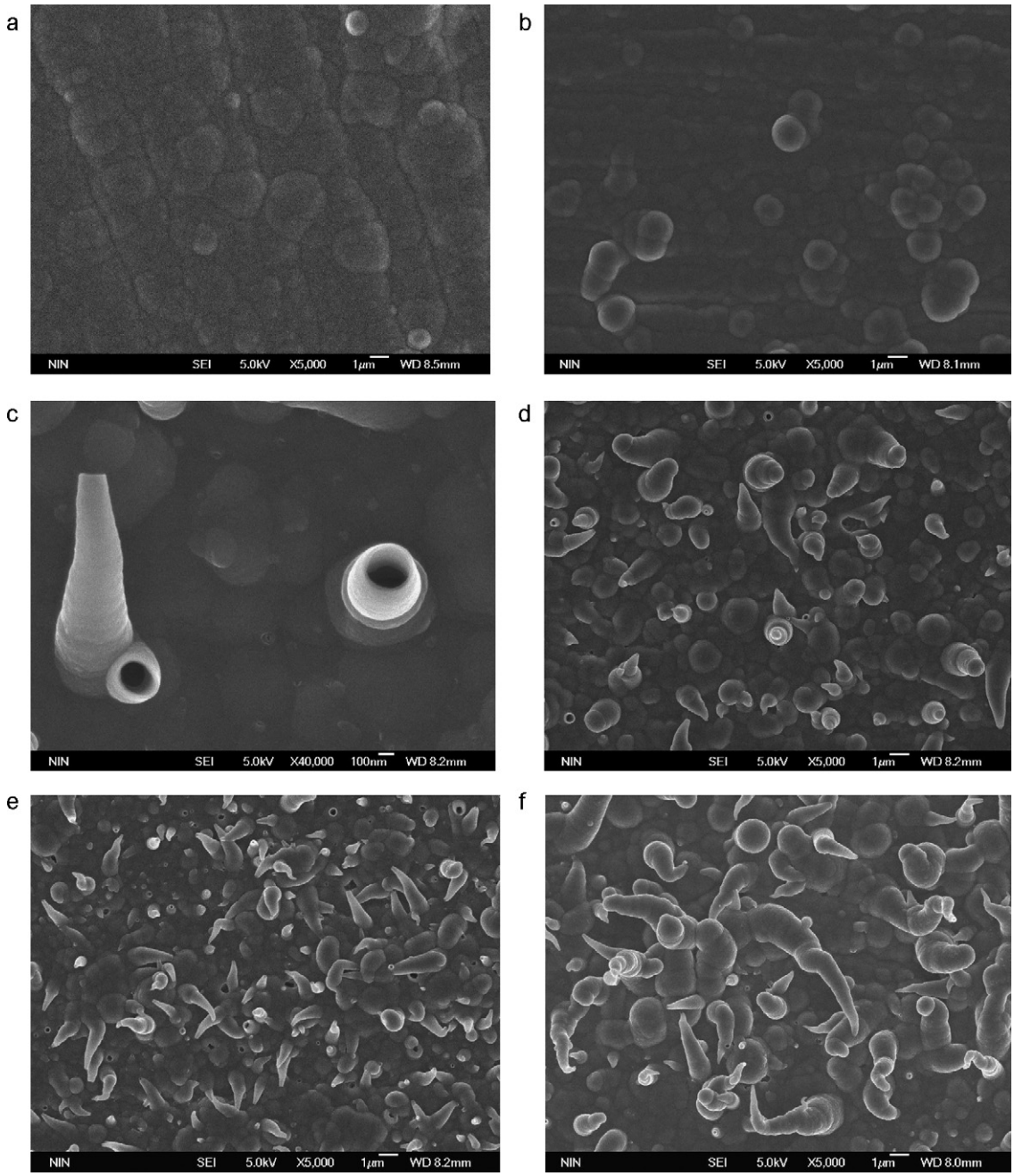

Fig. 2. SEM images of PPy films synthesized in various conditions, (a) TOS: 0.3 M, Py: 0.3 M, pH: 1.5, J: 5 mA cm^{-2}, (b) TOS: 0.1 M, Py: 0.1 M, pH: 9, J: 5 mA cm^{-2}, (c) TOS: 0.3 M, Py: 0.1 M, pH: 9, J: 5 mA cm^{-2}, (d) TOS: 0.3 M, Py: 0.1 M, pH: 9, J: 0.5 mA cm^{-2}, (e) TOS: 0.3 M, Py: 0.3 M, pH: 9, J: 3 mA cm^{-2} and (f) TOS: 0.6 M, Py: 0.6 M, pH: 9, J: 5 mA cm^{-2}.

TOS^- on the working electrode (Fig. 3(a)) acts as templates in forming PPy–TOS hollow horns (Fig. 3(b)), which has an analogy with β-NSA in composing PPy–NSA microctubes reported by Yang and Wan [28]. The inner diameter of microtubes in PPy–TOS gradually decreases during the growing process of horn, which results from TOS^-, the template, turning to join the polymerization as dopant (Fig. 3(c)). Finally, the end of horns closes when TOS^- is exhausted (Fig. 3(d)). The mechanism agrees well with the morphology transformation of h-PPy but is far from an exhaustive one. An intensive mechanism responsible for the entire formation of hollow horn still remains to be elucidated.

The structure of the novel h-PPy was examined by XRD analyses. Three diffraction peaks appear unexpectedly but evidently at positions A ($2\theta = 21.4^\circ$), B ($2\theta = 23.8^\circ$) and C ($2\theta = 26.6^\circ$), as shown by Fig. 4, which is a significant evolution because the conventional PPy is typically amorphous. To be concrete, the peak A is attributed to the pyrrole-counterion, the peak C results from interplanar spacing of the pyrrole chains, [33] and the peak at 39° from Ta substrate.

On the other hand, it is interesting that the length of crystalline domain of h-PPy films is up to 32.9 nm, calculated from Sherrer's formula,

$$L_{cd} = \frac{0.9\lambda}{(\Delta 2\theta)\cos\theta} \quad (1)$$

where $\Delta 2\theta$ represents the FWHM of Bragg angle 2θ. Generally, it is using weak current under low temperature that the highly ordered PPy can be synthesized. The maximal length reported of crystalline domain is 2.61 nm, obtained using low current density of 0.05 mA cm^{-2} at a temperature of −40 °C, [34] which is 10 times less than the value of h-PPy prepared in the facile condition (with

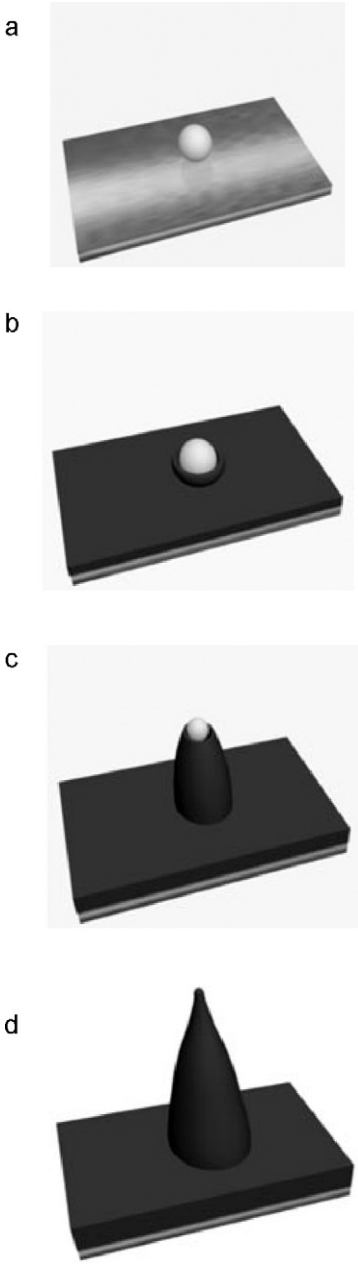

Fig. 3. Scheme showing the growth model of h-PPy, TOS^- micelle absorbed on the tantalum electrode (a), initial formation of h-PPy with TOS^- micelle as "template" (b), formation of h-PPy with open hollow horn (c), formation of h-PPy with closed end horn (d); silver gray: tantalum substrate, white: TOS^- micelle and gray: PPy.

high current density of 5 mA cm^{-2} in 0 °C solution). The high ordering of h-PPy formed by this method may arise from PPy growing preferentially along the electric field with the assistance of TOS^- template. The increased ordering in PPy can effectively improve the transport rate of ions in PPy electrodes and thereby elevate the charging/discharging rate.

Fig. 5 presents resonance Raman spectra of h-PPy, c-PPy as well as Ta, which does not show any valuable feature. The Raman spectra of h-PPy and c-PPy are only different in relative intensity of some Raman signatures. Prominent bands in Fig. 5(a)–(j) are: (a) 614 cm^{-1} (ring torsion); (b) 686 cm^{-1} (C–H wagging); (c) 880 cm^{-1} (ring deformation); (d) 937 cm^{-1} (ring deformation associated with dictation); (e) 1070 cm^{-1} (symmetrical C–H in-plane bending and N–H in-plane deformation); (f) 1236 cm^{-1} (antisymmetrical C–H in-plane bending); (g) 1370 cm^{-1} (antisymmetrical in-ring C–N stretching); (h) 1410 cm^{-1} (C–C and C–N stretching); (i) 1500 cm^{-1} (C–C and C–N stretching); and (j) 1590 cm^{-1} (C=C in-ring and C–C inter-ring stretching, which is an overlap of bands resulting from radical cation and dictation) [30].

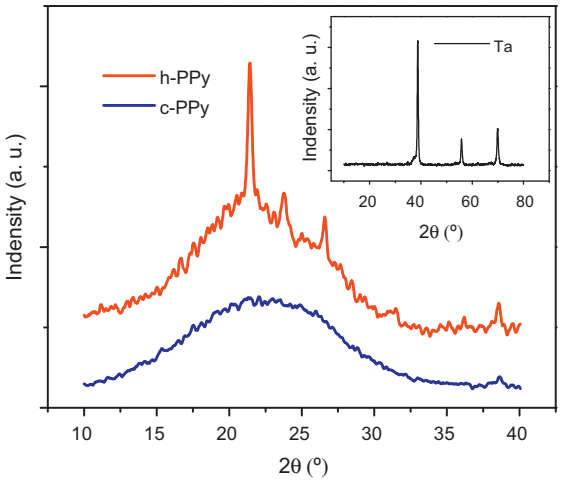

Fig. 4. X-ray diffraction spectra of h-PPy and c-PPy films as well as Tantalum electrode (up-right corner).

The relative conjugation length, determined by the ratio between the intensity of the (j) (oxidization state sensitive) to (i) (skeletal band), is calculated to be 2.56 and 1.74 for h-PPy and c-PPy, respectively. The greater conjugation length of h-PPy implies the higher polarizability, which is in direct correspondence with the increase of the room temperature conductivity (σ_{RT}). The σ_{RT} of free-standing h-PPy film reaches 90 S cm^{-1}, while that of conventional PPy prepared in the alkaline solution is even less than 10 S cm^{-1}. The longer conjugation of h-PPy may be related to its much higher ordering.

Electrochemical impedance spectroscopy (EIS), galvanostatical charging/discharging, and cyclic voltammetry (CV) tests were employed to evaluate the electrochemical characteristics of the novel material. Fig. 6 presents the EIS spectra of h-PPy and c-PPy with the same polymerization charge, and their specific capacitance (C_s) as the function of frequency. EIS spectrum indicates that h-PPy has ideal electrochemical capacitance behavior, i.e., imaginary part of impedance at low frequency region being perpendicular to the real part. Their EIS characteristics are shown in Table 2. h-PPy not only has far lower charge transfer resistance (R_{CT}), calculated from

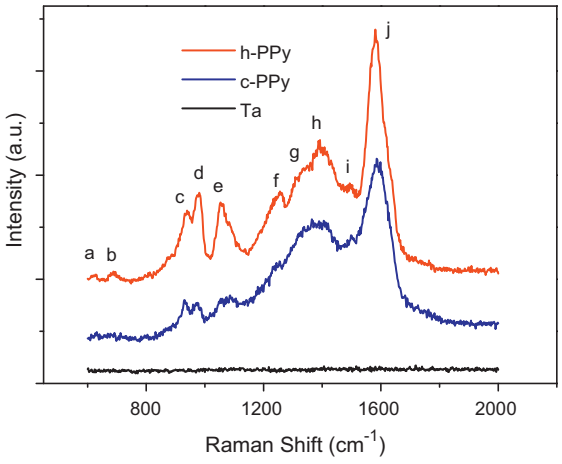

Fig. 5. Raman spectra of h-PPy (red line), c-PPy (blue line) and Ta (black line). (For interpretation of the references to color in this figure legend, the reader is referred to the web version of this article.)

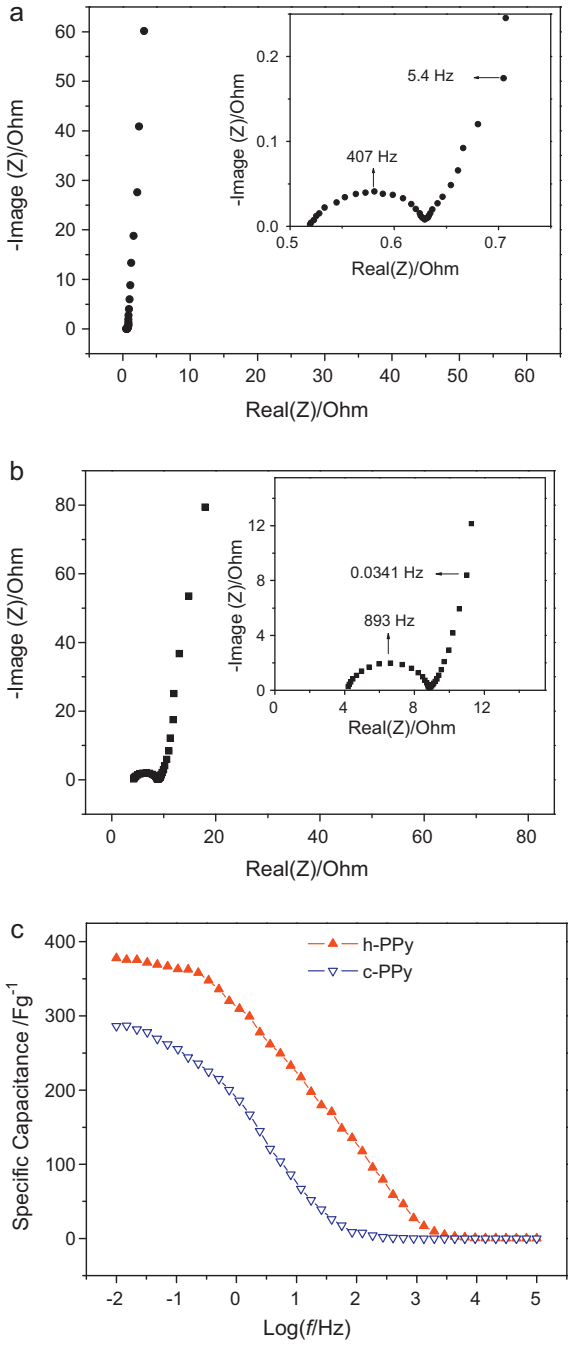

Fig. 6. EIS spectra of h-PPy (a) and c-PPy (b) in 3 M KCl solution and their specific capacitance as the function of frequency (c).

the difference in the real part of the impedance between low and high frequency, but also shows a higher knee-frequency (f_k), indicating an extraordinarily fast charging/discharging ability, since f_k is the maximal frequency at which predominant capacitive behavior can be maintained [35]. Furthermore, h-PPy exhibits greater C_s values, especially in high frequency region up to 100 Hz, evaluated

Table 2
Characteristics of c-PPy and h-PPy electrodes from EIS spectrum.

	C_s (10 mHz) ($F g^{-1}$)	C_s (1 Hz) ($F g^{-1}$)	R_{ct} (Ω)	f_k (Hz)	f^* (Hz)	S (cm^2)
c-PPy	380	220	4.7	0.0341	893	1.95
h-PPy	285	67	0.11	5.4	407	178

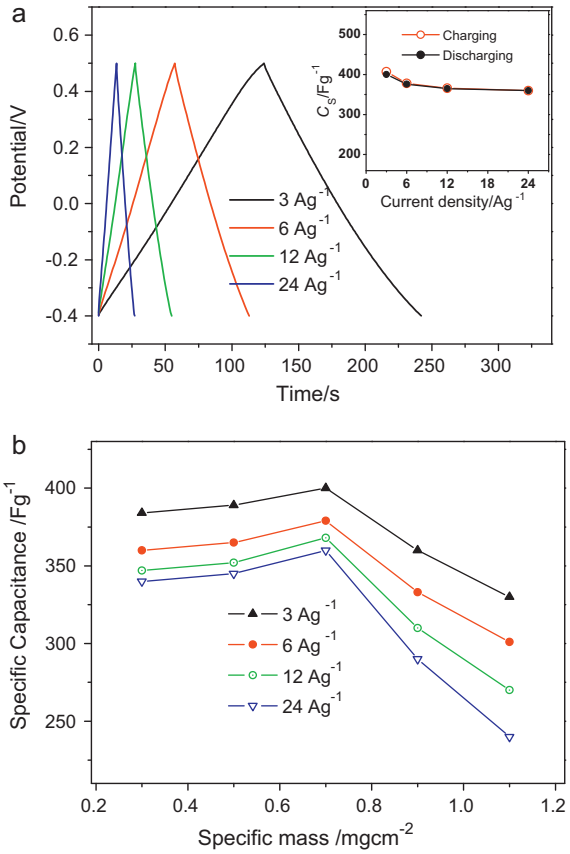

Fig. 7. Galvanostatical charging/discharging curves and specific capacitance (upper-right corner) of h-PPy electrodes in 3 M KCl solution (a) and specific capacitance of h-PPy electrodes with various masses (b).

by the Eq. (2),

$$C_s = \frac{-1}{2\pi f Z_{im} m} \quad (2)$$

where f represents frequency, Z_{im} is image (Z) and m is mass of PPy.

In addition, the surface area (S) of h-PPy is larger than that of c-PPy by 100 times. Firstly, the electronic double-layer capacitance (C_{dl}) is computed by the Eq. (3),

$$C_{dl} = \frac{1}{\omega * \times R_{ct}} \quad (3)$$

where ω^* is characteristic frequency. Then, S is estimated by C_{dl} dividing by the capacitance per cm^2 which is assumed as 20 μF cm^{-2} in KCl aqueous solution [3].

The hollow horn-like structure of h-PPy, significantly decreasing the transports length of ions and electrons, is the primary important reason why h-PPy exhibits high specific capacitance and rapid charging/discharging ability. Its high surface area, i.e., increased electrochemical accessibility to electrolyte, which also arouse from the horn-like structure, is another contribution factor. Besides, the ordering structure of h-PPy increases the transport rate of ions.

Fig. 7(a) shows the charging/discharging curves of h-PPy electrode at different current loads. All the curves, even at a load of 24 $A g^{-1}$ (the charging/discharging time of 13 s), are linear in the entire range of potential (−0.4 to 0.5 V vs SCE) without any obvious ohm-drop (IR-drop), indicating an ideal capacitance behavior again. The specific capacitance, as a function of current density, is displayed in the up-right part of Fig. 7(a). The discharging capacitance of the h-PPy is around 400 $F g^{-1}$ at a discharging current density of 3 $A g^{-1}$. Moreover, the capacitance retention is up to 90% when the current density increases from 3 $A g^{-1}$ to 24 $A g^{-1}$, suggesting a

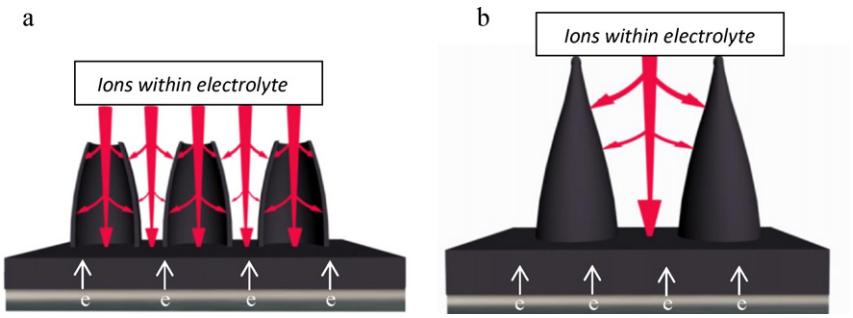

Fig. 8. Schematic representation of the increased surface area and reduced ion transport length of h-PPy with the open horns (a) and the closed horns (b); silver gray: tantalum electrode and gray: PPy.

good rate capability again, which is vital for the active material of supercapacitors to provide high power density.

The effect of mass on specific capacitance of h-PPy electrodes was examined. The specific capacitance increases with the rising specific mass at first, then decreases after a maximum value of 0.7 mg cm^{-2} (Fig. 7(b)). The first phase attributes to the increasing horns, which enables an easier access to electrolyte and thereby promotes plentiful ions to contact the surface of the active material. The second phase is caused by the over growing horns decreasing the ion accessibility. Not only the end of horns becomes closed, but also the tube wall of horns and the PPy films on Ta substrate turn thicker.

The high specific capacitance, fast charging/discharging ability and the effect of the mass of h-PPy electrodes are further discussed by the scheme of Fig. 8 and these two phases can also be clearly explained. The open hollow horns significantly increase the surface area of PPy by extending both outer and inner horn tubes (Fig. 8(a)). Meanwhile, the diffusion length (L) of ions in the PPy matrix is effectively reduced to half of the thickness of horn wall in nanometers, so the diffusion time (t) is remarkably shortened, according to the estimation of t as (L^2/D) where D is diffusion coefficient. h-PPy holds good specific capacitance and fast charging/discharging ability during this phase. After a turning point where h-PPy's mass was about 0.7 g cm^{-2}, as the polymerization goes on, these open horns become close as well as both horn wall and PPy film under it become thicker (Fig. 8(b)), resulting in the decrease of surface area and the increase of L to full horn-walled thickness. But even in this phase, h-PPy well outperformed c-PPy in all electrochemical properties [4].

The high specific capacitance and rapid charging/discharging ability of h-PPy electrode were further demonstrated by CV tests with scan rates ranging from 50 to 2000 mV s^{-1}. The response current is divided by the corresponding scanning rate and the mass of h-PPy films (0.7 mg) in Fig. 9, so that the shape of CV curves can be easily compared. All the CV curves are close to rectangle (Fig. 9(a)), indicating a remarkably fast kinetic process [36]. The specific capacitance of h-PPy reaches 390 F g^{-1} at the scanning rate of 50 mV s^{-1}, which is still up to 274 F g^{-1} even at 2000 mV s^{-1}, i.e., with the charging/discharging time of only 0.4 s (Fig. 9(b)). Besides, the coulombic efficiency (discharging capacitance/charging capacitance) is nearly 100%.

The electrochemical stability of the h-PPy was tested by CV cycling at a scanning rate of 500 mV s^{-1} with a potential window of 0.8 V, which means both charging and discharging time were 1.6 s. As for a h-PPy film weighted as 0.7 mg cm^{-2} (denoted as h-PPy-0.7 in Fig. 10), its maximal capacitance is 357 F g^{-1}, and surprisingly, still up to 324 F g^{-1} after 100,000 consecutive cycles, i.e., capacitance retains 90% after such a long term. To the best of our knowledge, it is the first report that polymer-based electrodes of supercapacitors are able to stably charge/discharge over 100,000 cycles.

As for another h-PPy film weighted as 0.3 mg cm^{-2} (denoted as h-PPy-0.3 in Fig. 10), its maximal specific capacitance is 328 F g^{-1}, and its stable cycles is about 25,000. The difference in stability is attributed to the greater proportion of "horns" in h-PPy-0.7 electrodes so that there are more hollow nanostructure of horns to tolerate and partake the volume scale change and the resulted strain during charging/discharging process. In spite of the difference in stability, the coulombic efficiency is close to 100% for both h-PPy-0.7 and h-PPy-0.3 thanks to their high electronic and ionic conductivity. With its outstanding stability and high coulombic efficiency, h-PPy can be considered as an excellent electrode material in cycling performance.

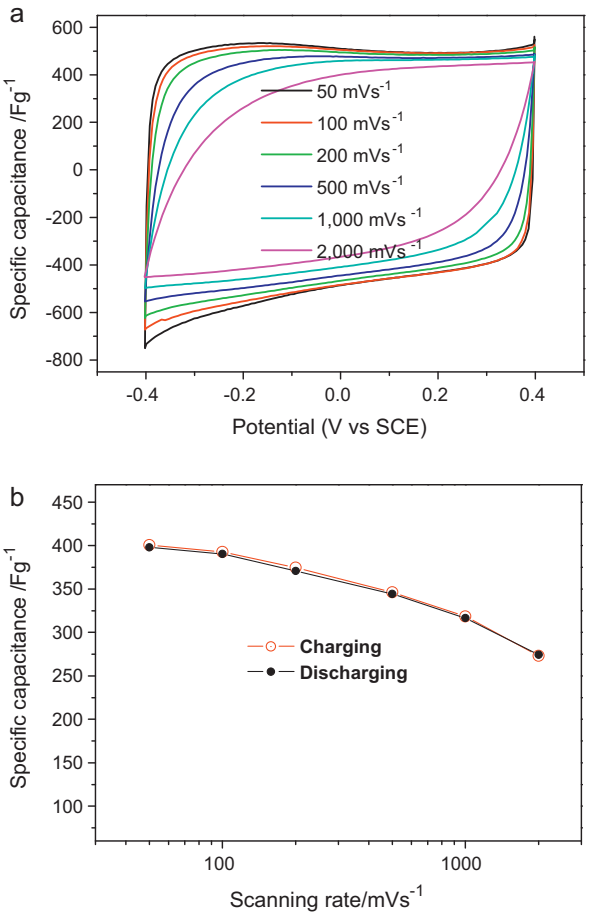

Fig. 9. Cyclic voltammograms (a) and specific capacitance (b) of h-PPy electrode at various scanning rates in 3 M KCl solution.

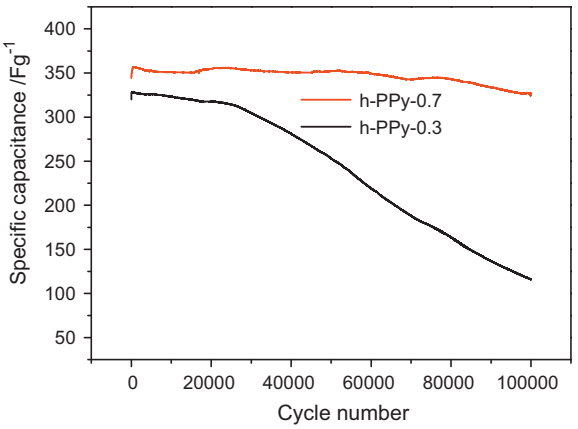

Fig. 10. Specific capacitance of h-PPy with various masses during the cycle test at a scanning rate of 500 mV s^{-1} in 3 M KCl solution.

4. Conclusions

The novel polypyrrole films with micro/nanometer-sized hollow "horns" are electrochemically synthesized by galvanostatical polymerization in alkaline solutions with TOS^- as dopant. Effect of the polymerization conditions (e.g. pH value of solution, concentration of TOS^- and pyrrole monomer, current density as well as polymerization time) on the morphology of the PPy was investigated. It is demonstrated that pH value and TOS^- concentration are essential in the formation of hollow horns. A growth mechanism is proposed according to the morphology transformation of horn that the absorbed TOS^- micelles act as templates with the assistance of OH^-. Other than the distinctly high surface area, h-PPy exhibits an unexpectedly good ordering of molecular chain with a crystalline length of 32.9 nm and an increased conjugation length, leading to remarkably high ionic and electronic conductivity. With all these advantages, h-PPy shows a great specific capacitance of 400 F g^{-1}, an ultrafast charging/discharging ability and a very stable cycling performance, which enable it to be an excellent active material for supercapacitors. Further work on an exhaustive formation mechanism responsible for the novel hollow "horns" morphology is underway.

Acknowledgments

The authors thank for the financial supports by the National Natural Science Foundation of China (Grant No. 20804030) and the National High Technology Research and Development Program of China (Grant No. 2007AA03Z249).

Appendix A. Supplementary data

Supplementary data associated with this article can be found, in the online version, at doi:10.1016/j.jpowsour.2010.10.066.

References

[1] P. Simon, Y. Gogotsi, Nat. Mater. 7 (2008) 845.
[2] M. Winter, R.J. Brodd, Chem. Rev. 104 (2004) 4245.
[3] B.E. Conway, Electrochemical Supercapacitors: Scientific Fundamentals and Technological Applications, Kluwer Academic/Plenum Publishers, New York, 1999.
[4] Y.G. Wang, H.Q. Li, Y.Y. Xia, Adv. Mater. 18 (2006) 2619.
[5] G.A. Snook, C. Peng, D.J. Fray, G.Z. Chen, Electrochem. Commun. 9 (2007) 83.
[6] J. Wang, Y.L. Xu, X. Chen, X.F. Du, J. Power Sources 163 (2007) 1120.
[7] G.A. Snook, G.J. Wilson, A.G. Pandolfo, J. Power Sources 186 (2009) 216.
[8] R.K. Sharma, A. Karakoti, S. Seal, L. Zhai, J. Power Sources 195 (2010) 1256.
[9] L.-Z. Fan, J. Maier, Electrochem. Commun. 8 (2006) 937.
[10] R.K. Sharma, A.C. Rastogi, S.B. Desu, Electrochem. Commun. 10 (2008) 268.
[11] L. Groenendaal, F. Jonas, D. Freitag, H. Pielartzik, R. Reynolds, Adv. Mater. 12 (2000) 481.
[12] C.C. Hu, X.X. Lin, J. Electrochem. Soc. 149 (2002) A1049.
[13] V. Gupta, N. Miura, Mater. Lett. 60 (2006) 1466.
[14] G.Z. Chen, M.S.P. Shaffer, D. Coleby, G. Dixon, W.Z. Zhou, D.J. Fray, A.H. Windle, Adv. Mater. 12 (2000) 522.
[15] K.H. An, K.K. Jeon, J.K. Heo, S.C. Lim, D.J. Bae, Y.H. Lee, J. Electrochem. Soc. 149 (2002) A1058.
[16] E. Frackowiak, V. Khomenko, K. Jurewicz, K. Lota, F. Beguin, J. Power Sources 153 (2006) 413.
[17] H.T. Ham, Y.S. Choi, N. Jeong, I.J. Chung, Polymer 46 (2005) 6308.
[18] J. Wang, Y.L. Xu, X. Chen, X.F. Sun, Compos. Sci. Technol. 67 (2007) 2981.
[19] J.Y. Kim, K.H. Kim, K.B. Kim, J. Power Sources 176 (2008) 396.
[20] J. Wang, Y.L. Xu, F. Yan, J.P. Wang, F. Xiao, J. Solid State Electrochem. 14 (2010) 1565.
[21] M. Acik, C. Baristiran, G. Sonmez, J. Mater. Sci. 41 (2006) 4678.
[22] L. Liu, Y.M. Zhao, Q. Zhou, H. Xu, C.J. Zhao, Z.Y. Jiang, J. Solid State Electrochem. 11 (2006) 32.
[23] S. Lee, M.S. Cho, J.D. Nam, Y. Lee, J. Nanosci. Nanotechnol. 8 (2008) 5036.
[24] C.R. Martin, Science 266 (1994) 1961.
[25] S.I. Cho, S.B. Lee, Acc. Chem. Res. 41 (2008) 699.
[26] A. Malinauskas, J. Malinauskiene, A. Ramanavicius, Nanotechnology 16 (2005) R51.
[27] M. Acik, G. Sonmez, Polym. Adv. Technol. 17 (2006) 697.
[28] Y.S. Yang, M.X. Wan, J. Mater. Chem. 11 (2001) 2022.
[29] L.T. Qu, G.Q. Shi, Chem. Commun. 2 (2003) 206.
[30] S. Gupta, Appl. Phys. Lett. 88 (2006) 063108.
[31] S. Shimoda, E. Smela, Electrochim. Acta 44 (1998) 219.
[32] S. Pouzet, A. Ricard, A. Boudet, Electrochim. Acta 36 (1991) 1953.
[33] K. Cheah, M. Forsyth, V.T. Truong, Synth. Met. 94 (1998) 215.
[34] C.O. Yoon, H.K. Sung, J.H. Kim, E. Barsoukov, J.H. Kim, H. Lee, Synth. Met. 99 (1999) 201.
[35] M. Hughes, G.Z. Chen, M.S.P. Shaffer, D.J. Fray, A.H. Windle, Chem. Mater. 14 (2002) 1610.
[36] S. Ghosh, O. Inganas, Adv. Mater. 11 (1999) 1214.